JOURNAL OF MATERIALS SCIENCE 39 (2004) 2689– 2697

Cyclic deformation behaviour of a nickel base alloy at elevated temperature

G. CHAI*, P. LIU*, J. FRODIGH‡
*Sandvik Materials Technology, *R&D and ‡Tube, 811 81 Sandviken, Sweden*
E-mail: guocai.chai@sandvik.com

Low cycle fatigue tests for a hot extruded Nickel base alloy tube material have been performed at room temperature and at 204°C. The alloy shows a normal hardening and softening cyclic stress-strain response at room temperature. At 204°C, however, the cyclic stress-strain response shows a strain hardening first, followed by a relatively stable stress and finally a secondary cyclic strain hardening. This stable stress disappears with increasing strain amplitude. The mechanisms of the secondary cyclic strain hardening have also been investigated by transmission electron microscopy (TEM). Besides dislocation multiplication, interactions between stacking faults and moving dislocations and between interstitial atoms and moving dislocations could also contributed to this secondary cyclic strain hardening. The formation of micro-twins during cyclic loading at 204°C and its influence on the cyclic stress-strain response were also discussed.
© *2004 Kluwer Academic Publishers*

1. Introduction

Nickel base alloy, Alloy 690, is mainly used for heat transfer tubing in light water reactor steam generators [1]. This alloy is considered to be immune to primary water stress corrosion cracking and has equal or superior stress corrosion cracking resistance to other steam generator tubing materials. It has be used in the environments where temperature can be up to 330°C [1] and strain controlled fatigue can also be one of the mechanisms for material degradation [2].

Temperature has a significant influence on the low cycle fatigue behavior in metal materials [3, 4], which can cause critical changes in cyclic stress-strain response [3–5]. Three temperature regions have been defined. At low temperatures (about $0.25T_m$, T_m-melting temperature), a rapid cyclic hardening is followed by a softening until a saturation peak stress is attained [3], or followed by a nearly stable stress-strain response [4]. At intermediate temperatures ($<0.5T_m$), the cyclic softening period is replaced by stable stress-strain response, and the saturation peak stress is increased [3, 6]. For some alloys, however, a monotonic cyclic hardening can be observed [4, 7]. At high temperatures ($>0.5T_m$), a rapid cyclic hardening is followed by a cyclic softening, or only a cyclic softening occurs [3, 4].

The influence of temperature on the stress-strain response is related to the dislocation substructures formed during cyclic loading at elevated temperatures [3, 6, 8, 9]. Armas *et al*. [3] reported that the dislocation structures could be transformed from the planar arrays at low temperature, and the cells with tangled walls at intermediate temperature to the sub-grains with well defined boundaries at high temperature. However, a structure transformation from cells (wavy slip character) at low temperature, via a predominantly planar slip at intermediate temperature to wavy slip again at high temperature has also been observed [8, 9]. A low stacking fault energy has been found to promote planar slip [7].

The purpose of this study is to investigate the influence of temperature and strain amplitude on the cyclic deformation behaviour of Alloy 690. The mechanisms of the observed secondary cyclic strain hardening have been discussed.

2. Material and experimental

The material used in this study was a hot extruded Alloy 690 (Sandvik Sanicro 69) tube material with an outer diameter of 66 mm and a wall thickness of 4 mm, having the following compositions (in wt%) 0.018C, 0.24Si, 0.26Mn, 29.5Cr, 0.28Ti, 10.48Fe and balance Ni. The material has a mean grain size of about 53 μm and the static mechanical properties are shown in Table I.

Flat-sheet fatigue specimen with rectangular cross section (3.5 mm in thickness and 7 mm in width) was used. The low cycle fatigue testing was performed under total strain control at room temperature (RT) and at 204°C. A symmetric push-pull mode with a sinusoidal waveform and a frequency of 0.15 Hz (6×10^{-4} up to 1.8×10^{-3}/s) was applied.

In order to investigate the cyclic deformation mechanism, discs with a diameter of 3 mm were taken from both the fatigue-tested specimens and as received

TABLE I Tensile properties of Alloy 690 at room temperature and 204°C

Temperature (°C)	E (GPa)	Rp0.2 (MPa)	R_m (MPa)	Elongation (%)
20	210	321	716	47
204	200	276	617	42

material for transmission electron microscope (TEM) investigation. Thin foils were polished using an electrolyte of 15% perchloride acid ($HClO_3$) in methanol and at 17 V and −30°C. In order to reduce the risk for surface absorption of carbon, the fresh thin foils were immediately inserted into sample holder and analysed. The dislocation structures were studied using a Jeol 2000-FX analytical transmission electron microscope (TEM/STEM) operating at 200 kV.

3. Results and discussion

3.1. Cyclic stress-strain response

The cyclic stress-strain response during low cycle fatigue represents the changes in peak tensile stresses with the number of cycles. Fig. 1 shows the stress-strain response from this test. At room temperature, Alloy 690 shows a normal cyclic hardening and softening response. Increase in strain amplitude increases both hardening and softening rate (Fig. 1a). At 204°C, however, the cyclic stress-strain response is quite different. In the beginning, the stresses increase with increasing number of cycles as expected, it then changes depending on strain amplitude. At small strain amplitude, it comes to a nearly stable stress at 10 to 100 cycles, and then the stress increases again with further cyclic strain until the specimen fails. This indicates that the alloy exhibits a secondary cyclic hardening (Fig. 1b). At high strain amplitude, however, a softening instead of stable stress has also occurred before the secondary cyclic hardening appears. The phenomenon of the secondary cyclic hardening at high temperature has rarely been reported in the literature [10].

If we use exponent constant ($\sigma = aN^n$, σ-stress, N-cycles, a-constant, n-exponent constant) to describe the cyclic strain hardening rate, we can get the influence of strain amplitude on the strain hardening for the 1st and the 2nd cyclic hardening, which is shown in Fig. 2. For the 1st cyclic hardening, increase in strain amplitude increases the hardening rate. This indicates that increase in dislocation density is the main mechanism for the first cyclic hardening. For the 2nd cyclic hardening, it is just the opposite. The hardening rate decreases with increasing strain amplitude. On the other hand, the hardening rate in the 2nd period is somewhat higher than that at the 1st period at small strain amplitude, but, the hardening rate in the 1st hardening period is higher than that of the 2nd period at high strain amplitude. Obviously, increase in temperature will increase annihilation of dislocations, which causes a decrease in hardening rate.

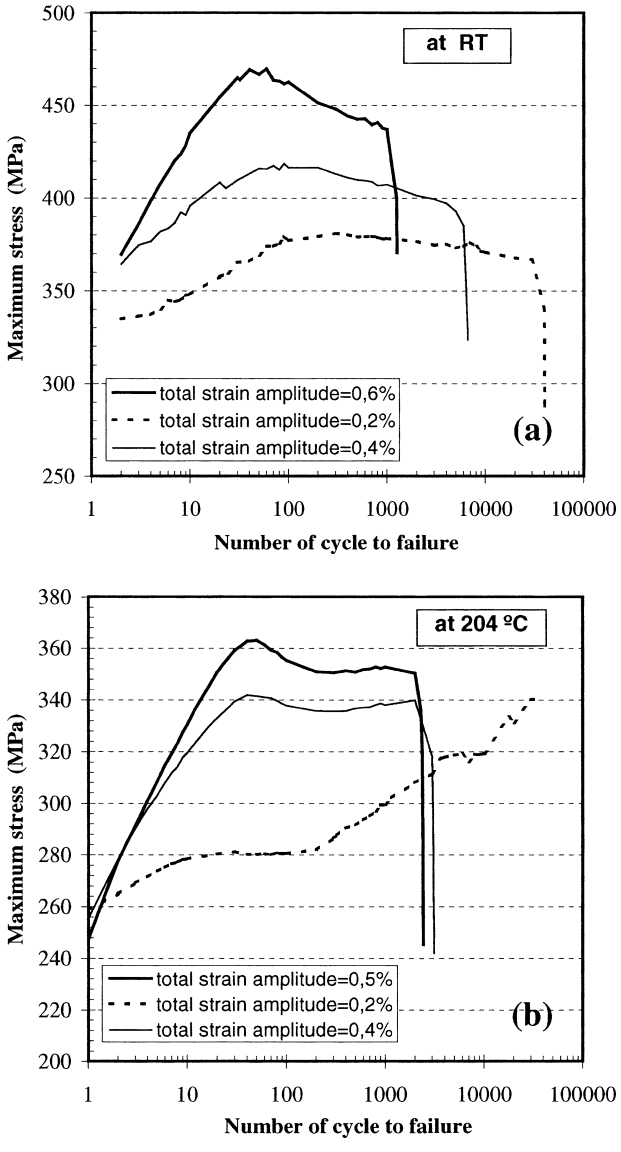

Figure 1 Effect of strain amplitude on the cyclic stress-strain response of Alloy 690 at room temperature and 204°C: (a) Stress-strain response at room temperature and (b) Stress-strain response at 204°C.

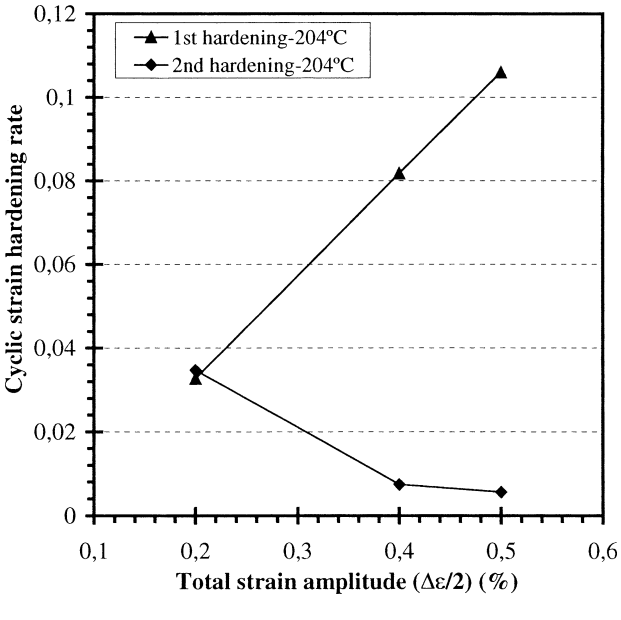

Figure 2 Influence of strain amplitude on the cyclic strain hardening rate in the 1st or 2nd cyclic hardening region.

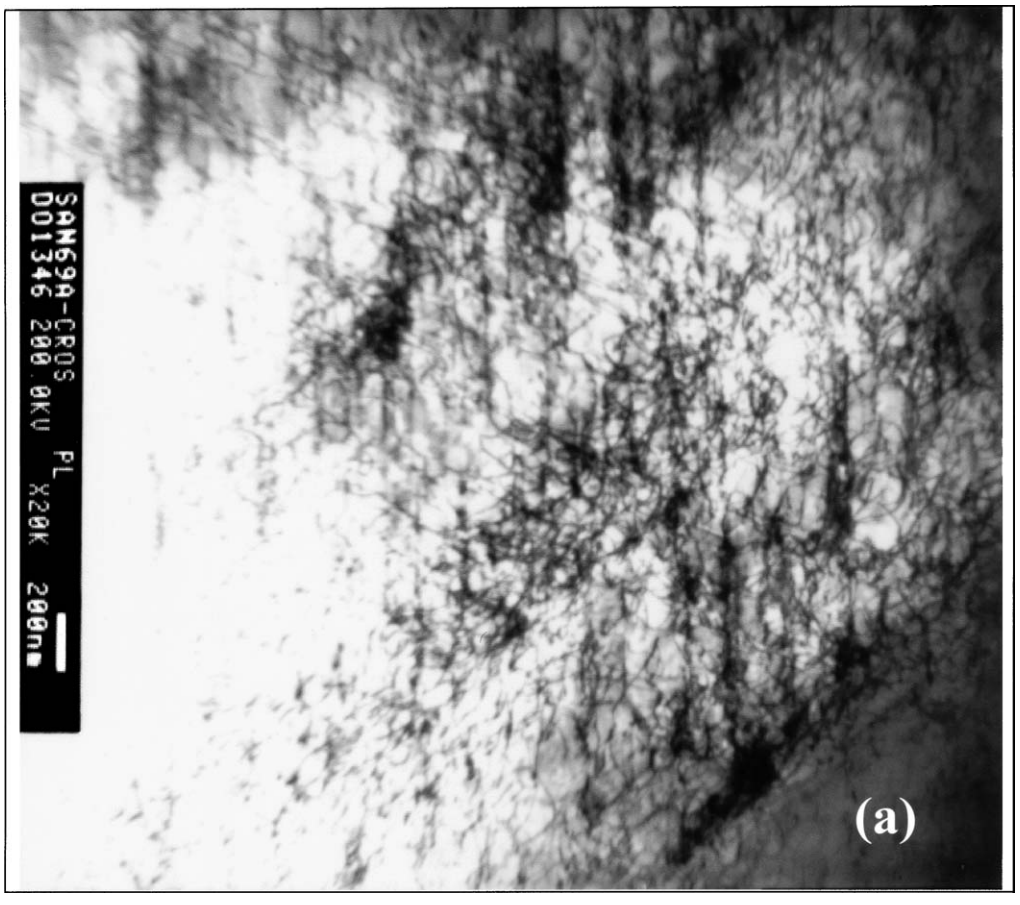

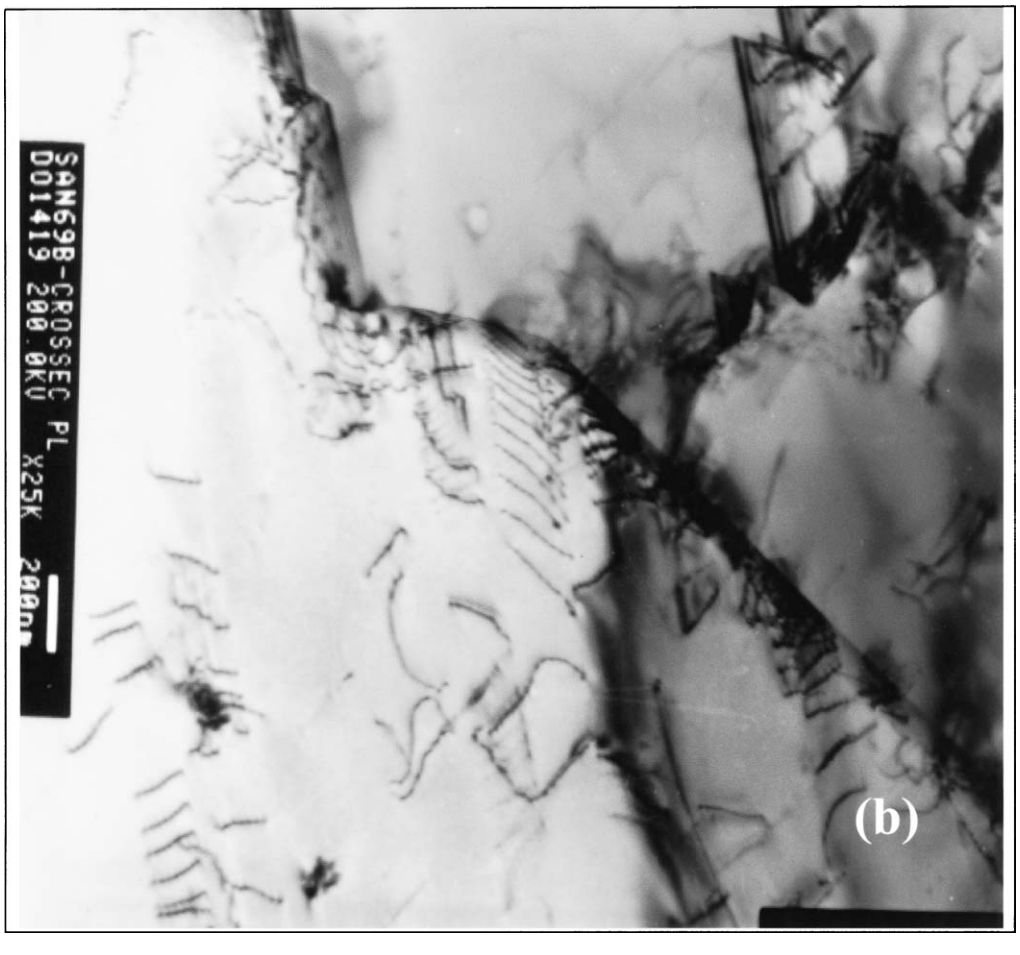

Figure 3 Dislocation structures in the Alloy 690 materials: (a) In the as received material and (b and c) In the specimen fatigue-tested with 0.2% total strain amplitude at 204°C, $N = 5$ cycles. (*Continued*)

Figure 3 (*Continued*).

Figure 4 Dislocation structures in the Alloy 690 material fatigue-tested with 0.2% total strain amplitude at 204°C, $N = 40000$ cycles.

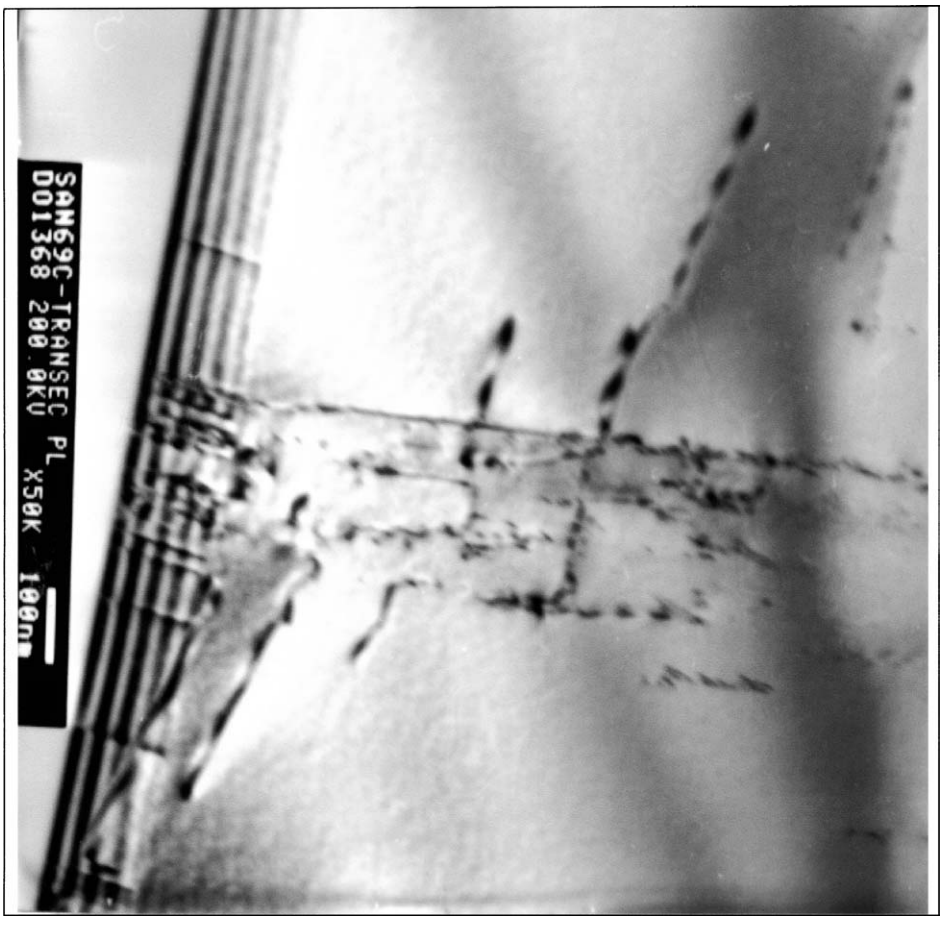

(a)

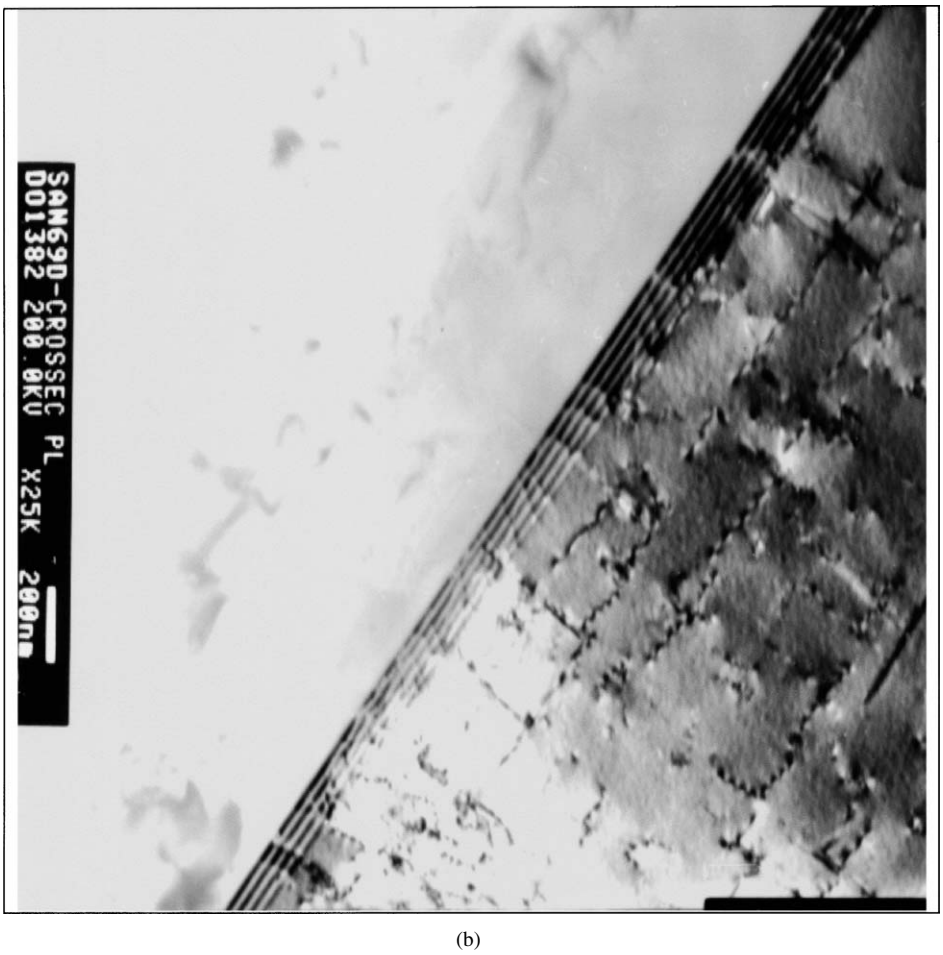

(b)

Figure 5 Interaction between stacking fault and moving dislocation: (a) In the specimen fatigue-tested with 0.2% total strain amplitude at 204°C, $N = 40000$ cycles and (b) In the specimen fatigue-tested with 0.5% total strain amplitude, $N = 2420$ cycles.

3.2. Possible mechanisms for secondary cyclic strain hardening

Transmission electron microscopy investigation shows that the as received material contains a dense dislocation structure (Fig. 3a), but the dislocation density decreases very quickly by initial few cycles (Fig. 3b). This can be explained by dislocation annihilation by reversed cyclic loading. At the same time, the new dislocations have been created, which are mainly confined in one glide plane and accumulated in the slip band oriented in the {111} directions (Fig. 3b and c). These results can be compared with that in copper single crystals where the dislocations produced by intial few cycles accumulate on the primary glide plane [11, 12]. This indicates that the cyclic strain hardening in the initial cycles is due to the dislocation multiplication and accumulation within the initiated slip band. With further fatigue cycling, the annihilation rate increases due to increasing dislocation density. This can lead to a progressive decrease in the strain hardening rate, and finally a state of saturation. Increase in temperature increases this annihilation rate.

For low strain amplitude, a well-developed planar array dislocation structure has been formed in the secondary cyclic strain hardening stage, and the dislocation density has also increased (Fig. 4). This certainly provides a contribution to the cyclic strain hardening. However, as shown in Fig. 2, the cyclic hardening rate in the 2nd hardening period is somewhat higher than that in the 1st hardening period at low strain amplitude. This may indicate that other mechanisms rather than dislocation multiplication may also have occurred during the 2nd cyclic hardening.

Although Alloy 690 has a high stacking fault energy, the stacking faults can still be observed in the fatigued specimen with both low and high strain amplitudes. The interactions between the moving dislocations and the stacking faults can often been observed in the specimens from the secondary cyclic strain hardening region (Fig. 5a and b). This phenomenon was earlier reported in one Cobalt based alloy, where monotonic cyclic strain hardening had occurred [4]. Obviously, this type of interaction will cause the difficulty to or even stop the movement of dislocations, which give a contribution to the strain hardening.

At elevated temperature, the interaction between the moving dislocations and the solute atoms is usually a mechanism for cyclic strain hardening in many alloys [2–5]. These phenomena are usually called the Portevin-LeChatelier effect or dynamic strain ageing [13]. Dynamic strain ageing refers to the phenomenon whereby certain materials exhibit an increase in yield and fatigue strengths over certain temperature ranges as a result of the interaction between dislocations and solute solution atoms. A typical characteristic is the serration along the stress-strain curve after a critical pre-strain. They can be determined by using different strain rates [14] or two double-twist flow curves [15]. Fig. 6 shows the serration stress-strain curves and the influence of temperature on the Portevin-LeChatelier effect in Alloy 690 at 204°C.

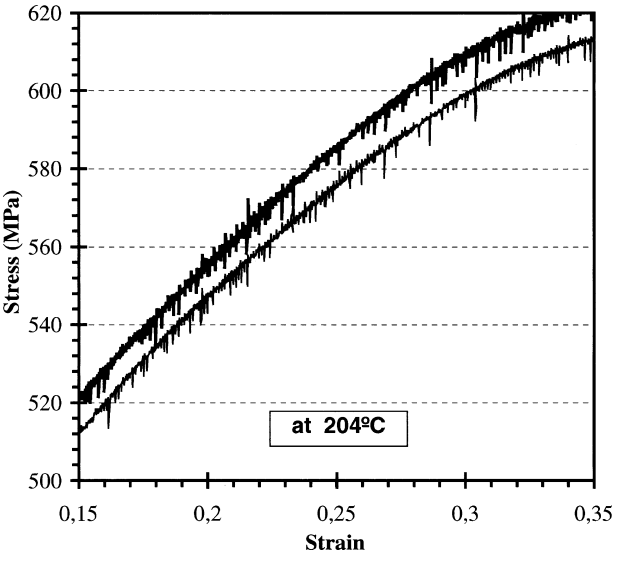

Figure 6 Typical serration stress-strain curves from one tensile test for Alloy 690 at 204°C.

Although dynamic strain ageing has been widely investigated, no direct evidence had ever been observed due to the difficulties. In this investigation, a large number of dark spots with a size of only a few nanometers have been observed along the boundary of dislocation arrays (Fig. 7a and b). They are interpreted as clusters of interstitial atoms trapped in the vacancies left behind by the dislocation movements. This type of cluster can also be observed in other places, but they are denser and larger along the boundary than in the matrix due to faster diffusion of interstitial atoms.

3.3. Cyclic softening by formation of micro-twins at high strain amplitude

At high strain amplitude, the dislocation structure is mainly planar array dislocation structure, and the dislocation lines orient in two different directions. However, its dislocation density (Fig. 8) is even lower than that at small strain amplitude (Fig. 4), and the secondary cyclic strain hardening rate decreases with increasing strain amplitude. This can not be explained by dislocation mechanism. Other deformation mechanism may have already started.

Transmission electron microscopy investigation shows that dense micro-twins with a width of $\sim$0.1 μm and distance between two micro-twins of $\sim$1–2 μm have been formed in the specimen with high strain amplitude in the secondary stain hardening region (Fig. 9a and b). Fig. 7a shows the dislocation lines oriented in the atomic planes of $(\bar{1}1\bar{1})$ in a single micro-twin. According to Murr *et al.* [16], micro-twins can initiate in Ni based alloy when the critical pressure is higher than 30 GPa. On the other hand, micro twinning can also initiate when easy dislocation glide is hindered [17]. In the present investigation, the formation of micro-twins may be attributed to these two factors since micro-twins have been observed at high strain amplitude and at high temperature where dynamic strain ageing and interaction between the moving dislocations and the stacking faults have occurred. The formation of micro-twins will contribute to most of the localised deformation. This

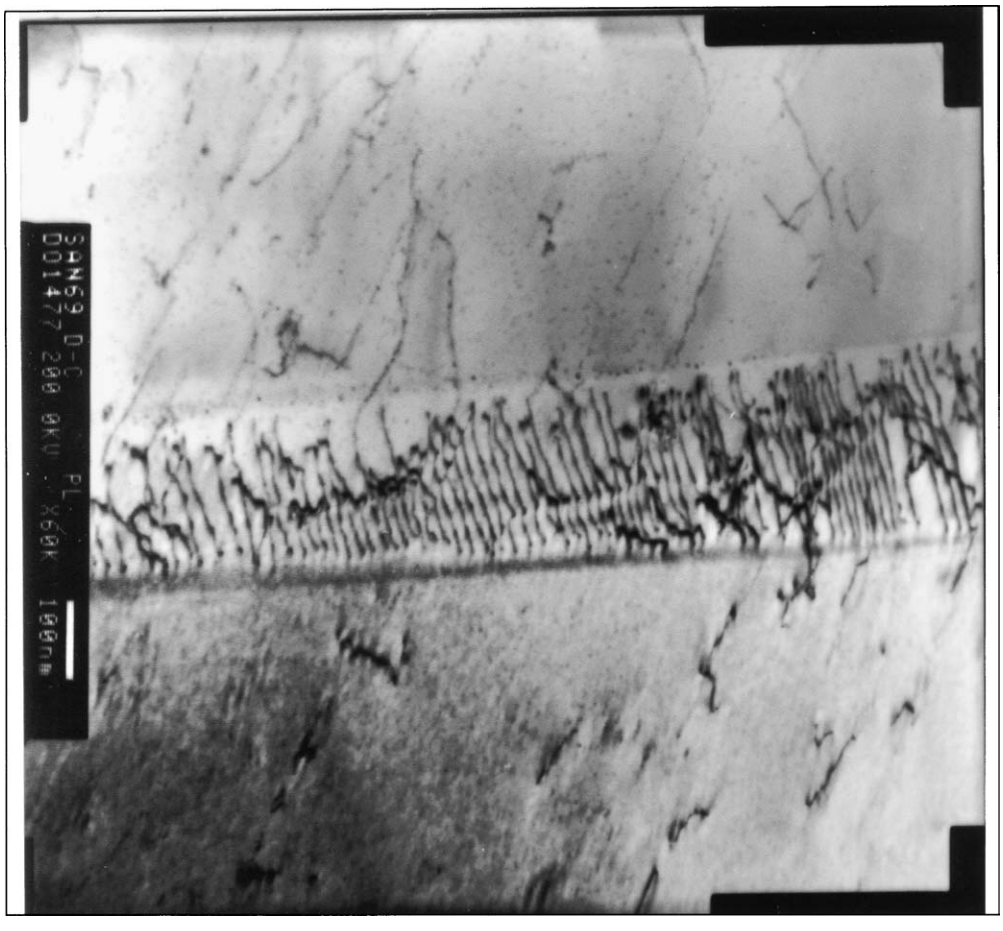

(a)

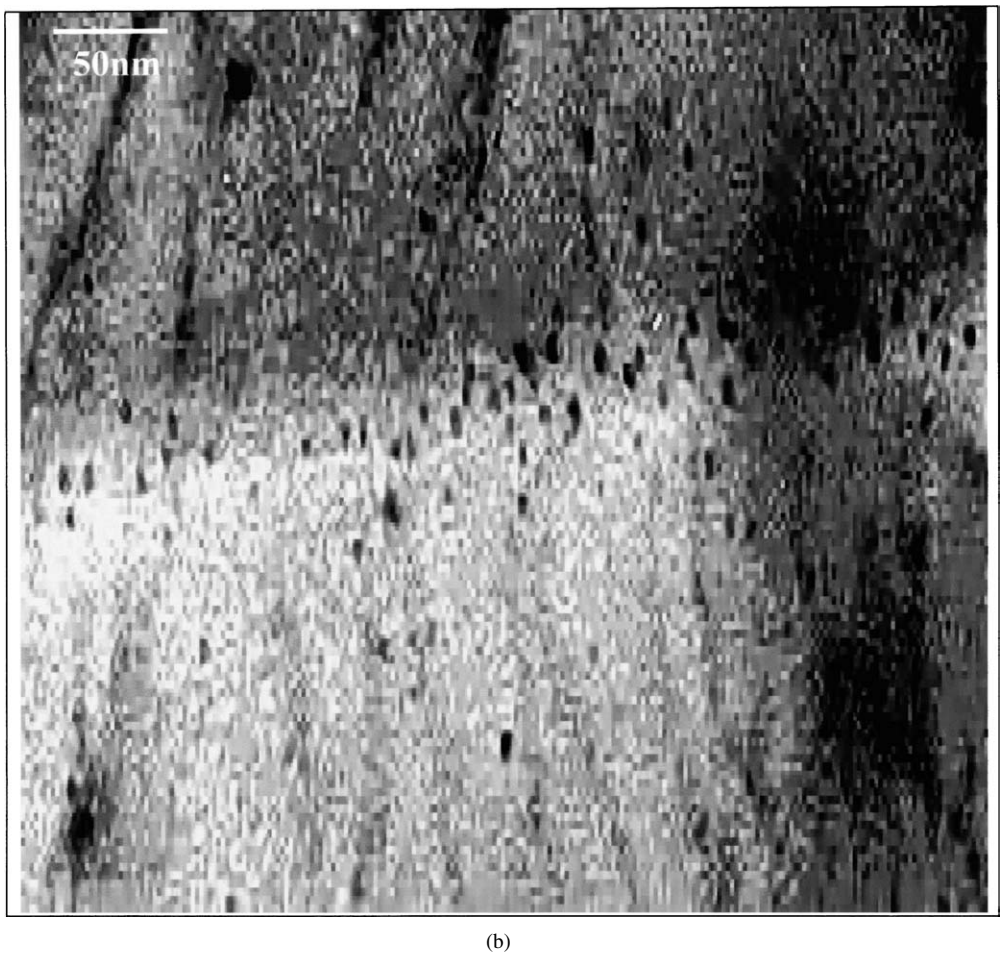

(b)

Figure 7 Dislocation structures in the specimen with 0.5% total strain amplitude, $N = 2420$ cycles: (a) Dislocation lines observed in one micro-twin and (b) Part of enlarged Fig. 7a; Note that a large number of dark particles with a diameter of a few nanometers along the walls of micro-twin.

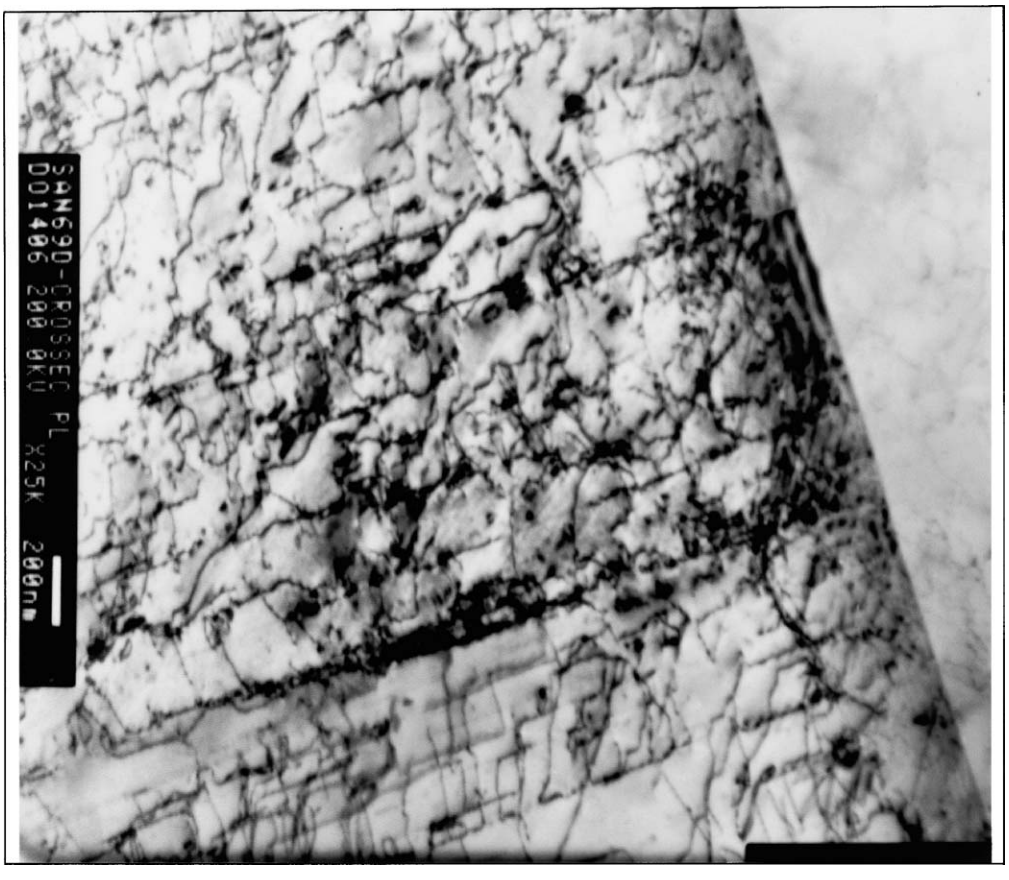

Figure 8 Dislocation structures in the Alloy 690 material fatigue-tested with 0.5% total strain amplitude at 204°C, $N = 2420$ cycles.

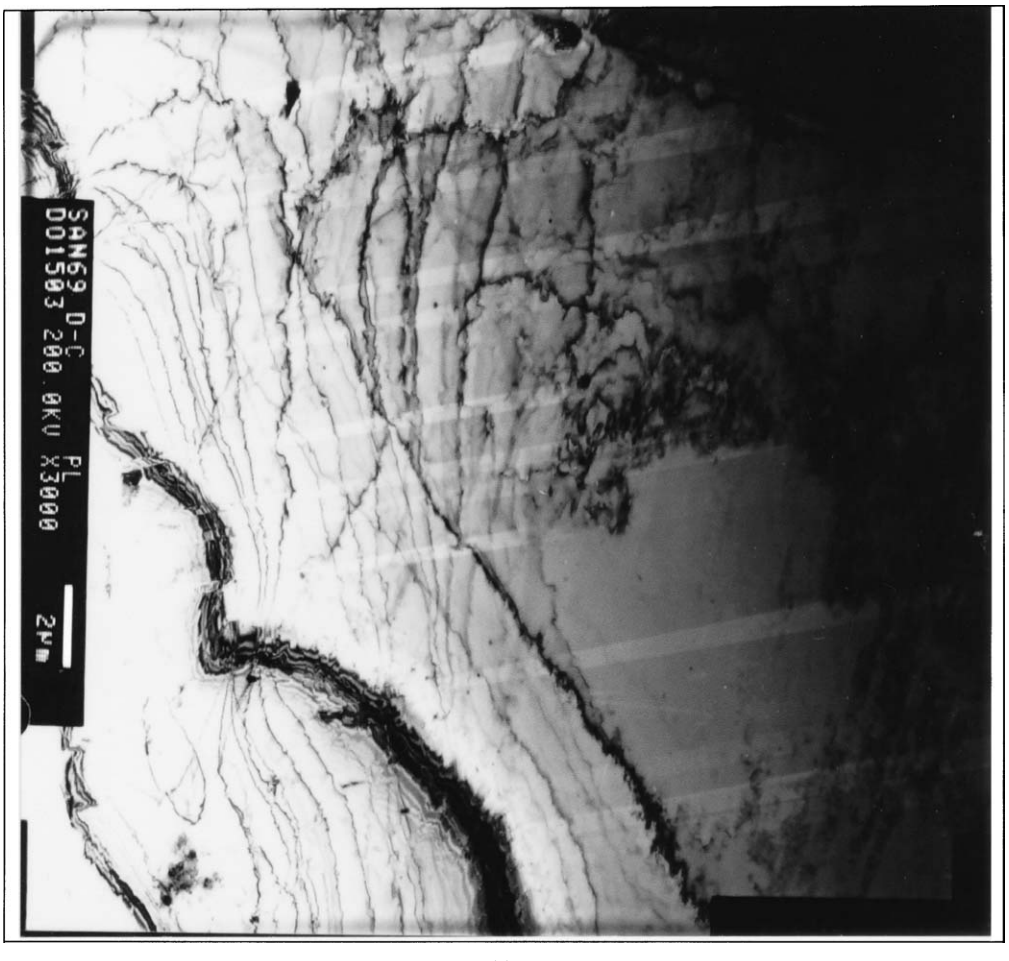

(a)

Figure 9 Micro-twins in the specimen with 0.5% total strain amplitude, $N = 2420$ cycles: (a) Micro-twins and (b) Electron diffraction pattern. (*Continued*)

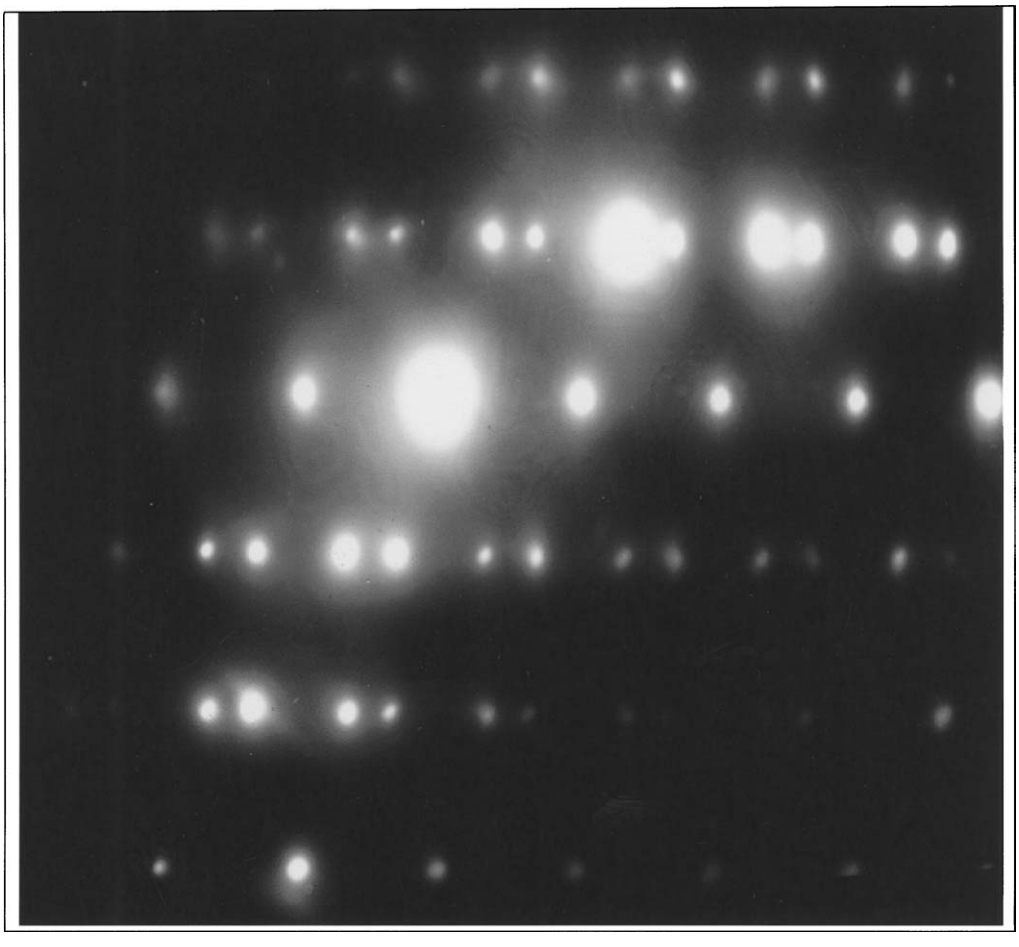

(b)

Figure 9 (*Continued*).

indicates that the softening at 204°C may be partly attributed to the formation of micro-twin, and partly due to the high rate of dislocation annihilation at high strain amplitude.

4. Conclusions

Hot extruded Alloy 600 shows a normal hardening and softening cyclic stress-strain response at room temperature. At 204°C, however, this alloy shows a secondary cyclic strain hardening, and the hardening rate decreases with increasing strain amplitude.

The secondary cyclic strain hardening occurred in a nickel base alloy at elevated temperature is attributed to the dislocation multiplication, interaction between stacking faults and moving dislocations and the Portevin-LeChatelier effect. The occurrence of cyclic softening at high strain amplitude is partly owing to the formation of micro-twins during cyclic loading.

Acknowledgements

This paper is published with permission of Sandvik Materials Technology. The support of Dr. T. Thorvaldsson, Prof., J. O. Nilsson, Mr. M. Lundström and Mr. H. Törnblom, and the technical assistance of Mr. G. Svensk are gratefully acknowledged.

References

1. D. L. HARROD, R. E. GOLD and R. J. JACKO, *JOM* July (2001) 14.
2. B. MUKHERJEE *et al*., *J. Nucl. Technol*. **55** (1981) 505.
3. A. F. ARMAS, O. R. BETTIN, I. ALVAREZ-ARMAS and G. H. RUBIOLO, *J. Nucl. Mater*. **155** (1988) 646.
4. M. VALSAN, K. B. S. RAO, M. G. CASTELLI and J. R. ELLIS, *Scripta Metall. Mater*. **33** (1995) 1005.
5. R. ZAUTER, F. PETRY, H. J. CHRIST and H.MUGHRABI, in "Thermomechanical Fatigue Behavior of Materials," ASTM STP 1186 (1993) p. 70.
6. M. VALSAN, D. H. SASTRY, K. B. S. RAO and S. L. MANNA, *Metall. Mater. Trans. A*. **25** (1994) 159.
7. J. O. NILSSON, *Scripta Metall. Mater.* **17** (1983) 593.
8. H. ABDEL-RAOUF, A. PLUMTREE and T. H. TOPPER, *Metall. Trans.* **5** (1974) 274.
9. K. D. CHALLENGER and J. MOTEFF, *ibid.* **3** (1972) 1675.
10. A. GIRONES, Ph.D Thesis, Universitat Politecnica de catalunya, Barcelona, Spain, 2003.
11. C. LAIRD, in "Physical Metallurgy," edited by R. W. Cahn and P. Haasen (North-Holland, 1996) p. 2294.
12. S. J. BASINSKI, Z. S. BASINSKI and A. HOWIE, *Phil. Mag*. **19** (1969) 899.
13. L. P. KUBIN, K. CHIHAB and Y. ESTRIN, *Acta Metall*. **36** (1988) 2707.
14. J. M. ROBINSON and M. P. SHAW, *Inter. Mater. Reviews* **39** (1994) 113.
15. S. CHO, Y. YOO and J. J. JONAS, *J. Mater. Sci*. **19** (2000) 2019.
16. L. E. MURR, C. NIOU, S. PAPPU, J. M. RIVAS and S. A. QUINONES, *Phys. Sta. Sol. (a)* **149** (1955) 253.
17. Z. W. HUANG and P. BOWEN, *Acta Metall. Mater.* **47** (1999) 3189.

Received 11 August 2003
and accepted 5 January 2004